Brain state-dependence of electrically evoked potentials monitored with head-mounted electronics

Andrew G. Richardson and Eberhard E. Fetz

***Abstract*—Inferring changes in brain connectivity is critical to studies of learning-related plasticity and stimulus-induced conditioning of neural circuits. In addition, monitoring spontaneous fluctuations in connectivity can provide insight into information processing during different brain states. Here, we quantified state-dependent connectivity changes throughout the 24-hr sleep-wake cycle in freely behaving monkeys. A novel, head-mounted electronic device was used to electrically stimulate at one site and record evoked potentials at other sites. Electrically evoked potentials (EEPs) revealed the connectivity pattern between several cortical sites and the basal forebrain. We quantified state-dependent changes in the EEPs. Cortico-cortical EEP amplitude increased during slow-wave sleep, compared to wakefulness, while basal-cortical EEP amplitude decreased. The results demonstrate the utility of using portable electronics to document state-dependent connectivity changes in freely behaving primates.**

***Index Terms*—primate, neural recording, stimulation, sleep**

I. Introduction

There is growing interest in artificially altering brain connectivity with electrical stimulation to improve recovery from brain injury [1]. Hebbian conditioning paradigms, in which targeted connections are strengthened or weakened by precisely timed activation of pre- and post-synaptic neuronal populations, have successfully modified connections in behaving animals and humans [2-7]. Integral to these studies is the measurement of conditioned changes in connectivity. Typically, the effects have been measured with an evoked behavioral output before and after the conditioning session or every few hours during extended sessions. Going forward, it is important to understand the evolution of the induced changes at a finer temporal resolution. Because chronic electrical stimulation can cause neural tissue damage [8], the dynamics of these changes could help determine a safe duration of conditioning sessions. Also, the time course of connectivity changes could be correlated with changing cognitive, behavioral, or pharmacological states to efficiently assay the states that maximize the conditioning effect. Finally, to better evaluate the induced changes, it is important to understand the time course of naturally-occurring fluctuations, in the absence of any conditioning stimuli. Here, we studied the use of a neural connectivity measure and a stimulus-recording system that together provide greater temporal resolution of connectivity changes in a primate during free behavior.

Specifically, we used electrically evoked potentials (EEP) to assess neural connectivity, where both electrical stimulation and evoked-potential recording were performed by a portable electrophysiology system housed on a monkey's head. The use of EEPs as a measure of connectivity has a long history in animals [9] and has more recently been used in humans [10-11], although this method does have some limitations [12]. Unlike previous EEP studies, our portable electronics allowed us to monitor EEPs in monkeys during free behavior throughout the day and night. Thus dynamic changes in connectivity could be documented, whether those changes resulted naturally from different brain states or artificially from conditioning paradigms like those mentioned above. The objective of the present work was to study normal EEP modulation throughout the 24-hour sleep-wake cycle. The results provide important insight into spontaneous state-dependent changes in brain connectivity. Furthermore they indicate the natural variability in EEPs which must be accounted for in future studies of the dynamics of artificially-induced connectivity changes.

Manuscript received August 1, 2011; revised April 18, 2012. This work was supported by NIH grants NS12542 and RR00166, the American Heart Association, the Life Sciences Discovery Fund, and the W. M. Keck Foundation.

A. G. Richardson and E. E. Fetz are with the Department of Physiology and Biophysics and with the Washington National Primate Research Center, University of Washington, Seattle, WA 98195 USA.

Color versions of one or more of the figures in this paper are available online at http://ieeexplore.ieee.org.

Digital Object Identifier

II. Methods

A. Animal preparation

All procedures were approved by the University of Washington Institute for Animal Care and Use Committee. The experiment was performed in two male pigtailed macaques (*Macaca nemestrina*), designated monkeys C and K. In each monkey, a sterile surgery was performed to implant intracranial electrodes and a skull-fixed titanium chamber in which electronics could be housed. In monkey C, six burr holes (0.8 mm diameter) were made through the skull with a stereotaxic drill to access the primary motor cortex (M1), supplementary motor area (SMA), and basal forebrain (BF) of both hemispheres. A concentric bipolar electrode with 0.5 mm

contact separation (NEX-100, David Kopf Instruments, Tujunga, CA) was implanted at each site, with the distal contact at a nominal depth of 2 mm (M1 and SMA) or 26 mm (BF). The electrodes and a 63 mm diameter titanium chamber centered around the implant sites were secured to 12 skull screws with acrylic. Monkey K had the same implants as monkey C, except only one BF electrode (right hemisphere) was implanted. The experiment began two weeks after the surgery.

B. Head-mounted electrophysiology system

A custom, battery-powered electronic device was used to electrically stimulate and record through the implanted electrodes. The device, called the Neurochip-2 [13], was small enough to fit inside the head-fixed titanium chamber and could execute a variety of recording and stimulating paradigms autonomously. This permitted us to evoke and monitor EEPs continuously while the monkey was behaving freely in its home cage.

As described in detail elsewhere [13], the Neurochip-2 has three independent AC-coupled differential recording channels with selectable gains and filters and three independent bipolar stimulating channels with ±15V compliance. Two programmable-system-on-chips (PSoCs, Cypress Semiconductor, San Jose, CA) controlled the data acquisition and stimulus output. The bipolar field potential recordings in this study were filtered between 1Hz-1kHz or 10Hz-1kHz and sampled at 2kS/s. The PSoCs wrote the data to an onboard 1-GB microSD flash memory card. The bipolar stimuli used in this study were square, biphasic, charge-balanced pulses of 0.2ms/phase duration and 0.75 to 1.0mA intensity. The PSoCs were programmed to deliver the stimuli at fixed intervals (1/min or 1/10min) while continuously recording the field potentials. The stimulation rates were chosen to provide good temporal resolution but not induce plasticity [5]. The electronics were powered by a rechargeable, 3.6V lithium-ion battery that was housed in the polycarbonate cap of the titanium chamber. The size of the assembled circuit boards was 20mm x 35mm x 55mm and the total weight including the battery was 145g.

C. Analysis

Two time-resolved features were computed off-line from each field potential recorded by the Neurochip-2: the EEP and the power spectral density (PSD). EEPs were computed over stimulus-triggered windows of -10ms to 40ms relative to stimulus onset. PSDs were computed in 1-s windows using Thompson's multitaper method. To improve the signal-to-noise ratio and reject outliers, the median of both the EEPs and PSDs were computed within a sliding 30 minute window to generate the final time-resolved features. The PSDs had the typical $1/f^x$ distribution of power [14]. The z-score of the power at each frequency was used to visualize relative changes in power over time.

For the purpose of this analysis, the PSD defined the brain state during the sleep-wake cycle. To relate EEP changes to brain state, correlation coefficients were computed between the EEP and PSD for selected EEP peaks and all PSD frequencies (1-100Hz), as described below.

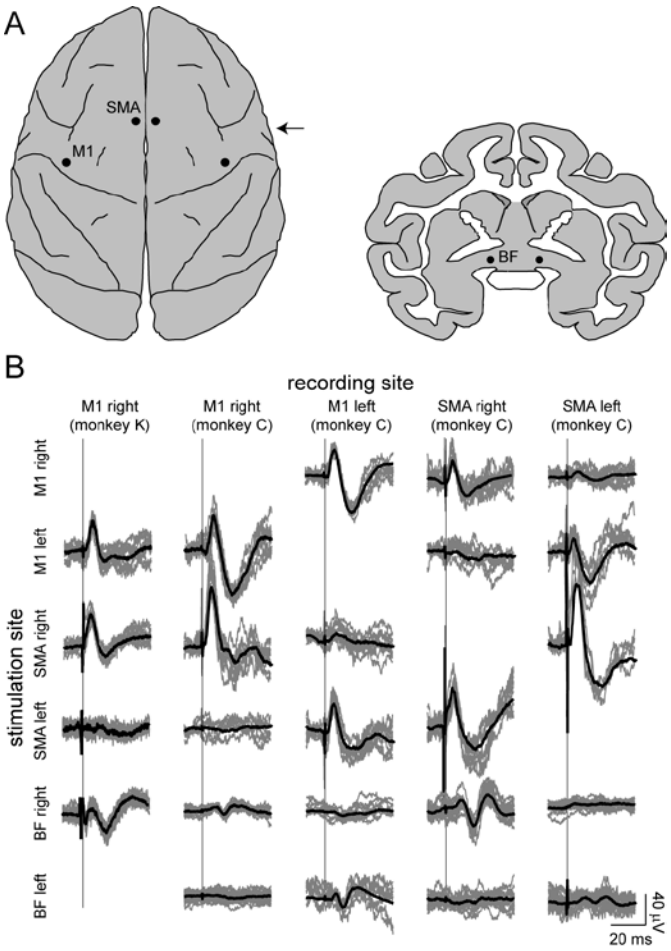

Fig. 1. EEP-based connectivity. (A) Schematic of the six sites implanted with bipolar electrodes (indicated by black circles). The arrow marks the approximate anterior-posterior position of the coronal brain slice drawn on the right. M1 = primary motor cortex; SMA = supplementary motor area; BF = basal forebrain. (B) Connectivity matrix between the six sites, as tested on one day approximately two weeks after the electrodes were implanted. Data from monkey K is in the 1st column. Data from monkey C is in the 2nd through 5th columns. The black traces are an average of the 15 to 25 stimulus-triggered sweeps shown in gray. Vertical lines mark the time of stimulus onset.

III. RESULTS

A. EEP-based connectivity

Bipolar electrodes were implanted into M1, SMA, and BF of both the left and right hemisphere (Fig. 1A; only BF right was implanted in monkey K). With the monkeys in a consistent state of quiet wakefulness, EEPs were used to determine how the implanted sites were connected. Stimuli were delivered to one site and field potentials were recorded at the other sites. An EEP-based connectivity matrix for monkey C is shown in Figure 1B (second through fifth columns). Stimulation at each of the four cortical sites failed to yield EEPs at the BF sites, so those two columns of the connectivity matrix were omitted

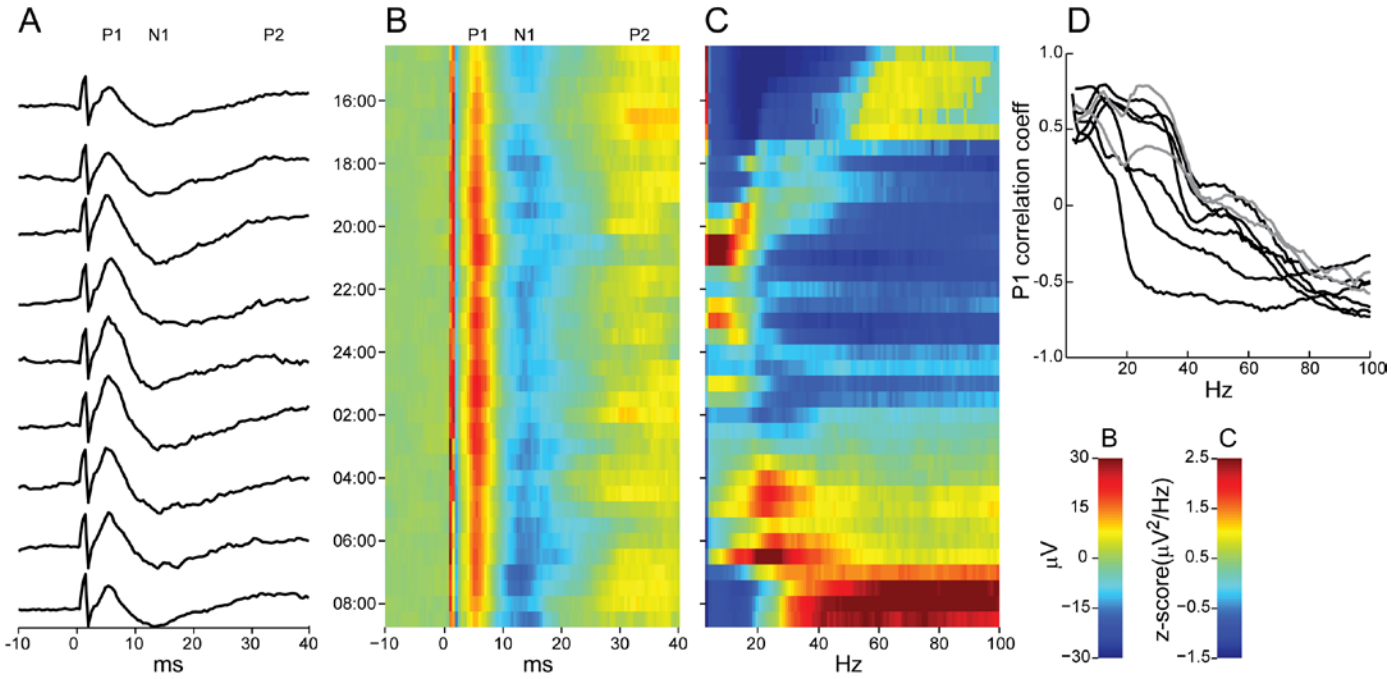

Fig. 2. State dependence of cortico-cortical EEPs. (A) Example EEPs from stimulating M1 right and recording SMA right in monkey C. Time is relative to stimulus onset. P1, N1, and P2 mark the three components of the EEP. (B) Same as in A, but showing the entire, time-resolved EEP trajectory for this recording. The amplitude scale is the left scale bar under panel D. The ordinal axis tick mark labels indicating time of day apply to plots A and C as well. (C) Time-resolved PSD for the same recording as in A and B. The relative power scale is the right scale bar under panel D. (D) Frequency-dependent correlation between the P1 component amplitude and PSD power for all cortico-cortical sessions (black = monkey C; gray = monkey K).

from Figure 1B. Only a subset of the connectivity matrix was obtained for monkey K (Fig. 1B, first column), since three of the four cortical electrodes (all but M1 right) failed to yield usable recordings. The spectra of these recordings differed significantly from that of M1 right in monkey K and that of all the cortical sites in monkey C (data not shown). Also, the stimulus artifacts were larger. Although a post-mortem evaluation has not been conducted in monkey K due to his use in ongoing studies, we hypothesize that the tips of these three electrodes were not at the appropriate depth in the cortex and may have been in the cerebrospinal fluid above the cortex. Nevertheless, stimulation through these electrodes was effective in generating EEPs (Fig. 1B, first column). Thus implant accuracy was more critical for recording than stimulating in this paradigm, as might be expected given the mA-range intensities used for the latter.

Stimulation of M1 right resulted in relatively large EEPs at M1 left and SMA right and a small EEP at SMA left (Fig. 1B, first row). Similarly, stimulation of M1 left evoked a large potential at M1 right and SMA left, but not at SMA right (Fig. 1B, second row). Thus there were strong connections between ipsilateral sites and homologous contralateral sites, but not heterologous contralateral sites. This same pattern was observed when stimulating SMA right and left (Fig. 1B, third and fourth rows).

While cortical stimulation failed to evoke potentials in the BF, the converse connection was evident. Stimulation of BF right resulted in EEPs at SMA right and M1 right, but not at the contralateral cortical sites (Fig. 1B, fifth row). Similar, ipsilateral connectivity was observed when stimulating BF left (Fig. 1B, sixth row). In summary, EEPs revealed a number of connections between the six brain areas during quiet wakefulness. The next step was to document how EEP size changed throughout a 24-hour, sleep-wake cycle.

B. State-dependence of EEPs

To assess how brain state influenced the strength of the connections described above, the head-mounted Neurochip-2 was programmed to deliver one stimulus every minute and to record field potentials continuously over a period of 18-24 hours while the monkey was behaving freely in his home cage. Eleven such Neurochip-2 sessions were conducted to test the cortico-cortical (six sessions) and basal-cortical (five sessions) connections in monkey C. Four sessions (two cortico-cortical, two basal-cortical) were conducted in monkey K.

A typical example of changes in the cortico-cortical EEPs is shown in Figure 2A. The median evoked potential, calculated over 30 min windows, is shown for every two hours of the recording. There was an increase in amplitude of the first component of the EEP, designated P1, during the night (particularly 20:00 – 04:00) followed by a decrease to its initial size by 8:00 the next morning. The entire set of responses over the 18-hr recording is shown in Figure 2B.

Throughout this experiment, the monkey was entrained to a 12:12 light-dark cycle with the 12-hr dark period occurring between the hours of 18:00 and 06:00. Clearly, in this example, the EEP amplitude increased mostly, but not exclusively, during the dark period. However, this analysis does not directly indicate whether the EEP changes were correlated to the sleep-wake cycle. To estimate these brain state changes, the median

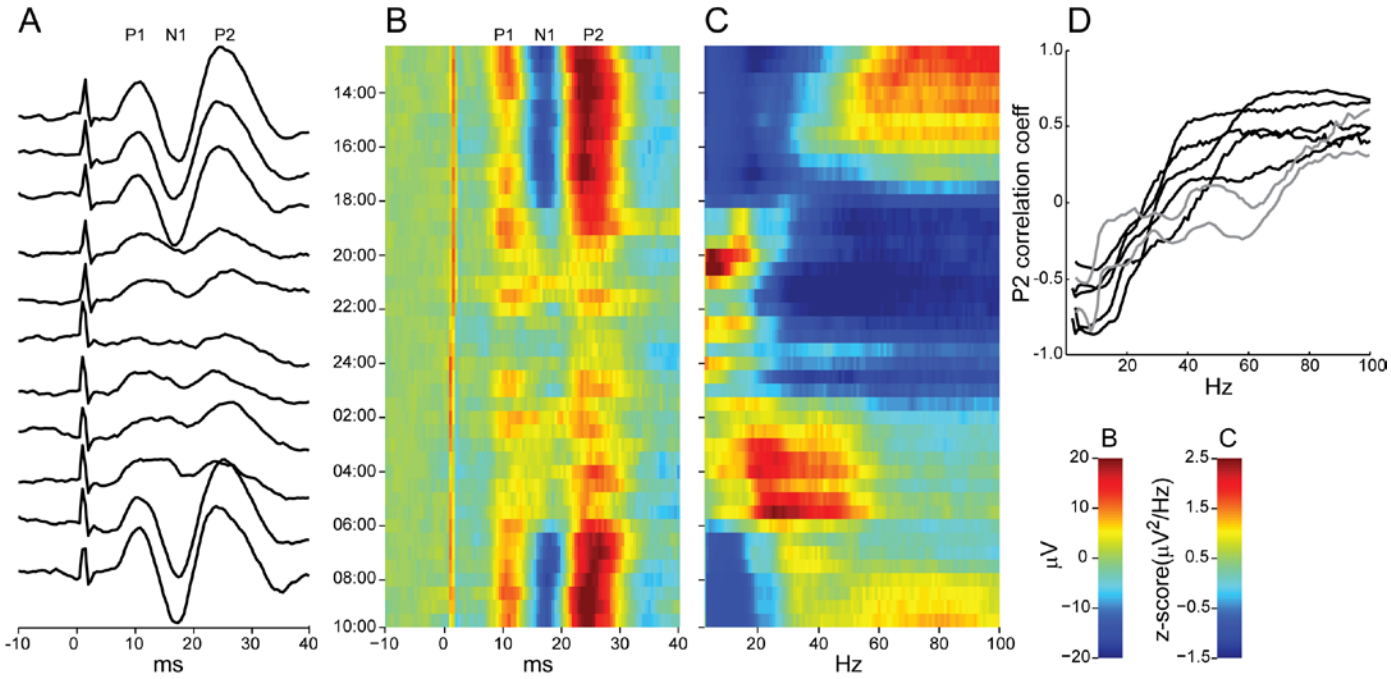

Fig. 3. State dependence of basal-cortical EEPs. (A) Example EEPs from stimulating BF right and recording ipsilateral SMA. Time is relative to stimulus onset. P1, N1, and P2 mark the three components of the EEP. (B) Same as in A, but showing the entire, time-resolved EEP trajectory for this recording. The amplitude scale is the left scale bar under panel D. The ordinal axis tick mark labels indicating time of day apply to plots A and C as well. (C) Time-resolved PSD for the same recording as in A and B. The relative power scale is the right scale bar under panel D. (D) Frequency-dependent correlation between the P2 component amplitude and PSD power for all basal-cortical sessions (black = monkey C; gray = monkey K).

PSD was computed from the recorded field potential in 30-min windows (Fig. 2C). The PSD varied substantially over the 18 hours with at least two prominent power distributions: relatively high power at high frequencies (>40Hz), characteristic of an awake state, and relatively high power at low frequencies (<10Hz), characteristic of a slow-wave sleep state. Thus, the increased EEP amplitude appeared to be correlated with the sleep state. To quantify the relationship between the EEP changes and brain state for all cortico-cortical sessions, correlation coefficients were computed between the P1 component of the EEP and each frequency of the PSD (Fig. 2D). In every case, the P1 amplitude was positively correlated with frequencies below 20Hz and negatively correlated with higher frequencies.

The same analysis was performed for the sessions that documented basal-cortical connections. A much more dramatic change in the EEP, involving all three components (P1, N1, and P2), was observed across the sleep-wake cycle for these connections (Fig. 3A, B). Interestingly, the sleep state was correlated with an EEP decrease rather than the increase observed in cortico-cortical connections (Fig. 3B, C). For each of the sessions, the P2 amplitude was negatively correlated with frequencies below 20Hz and positively correlated with frequencies above 40Hz (Fig. 3D).

C. Characterizing basal-cortical connections

As demonstrated in Figures 2 and 3, sleep-wake changes in EEP amplitude were common in both cortico-cortical and basal-cortical connections. The striking difference in polarity and degree of changes in the basal-cortical connections led us to further investigate the nature of these connections. Particular areas of the BF, most prominently the nucleus basalis, contain cholinergic neurons that project widely to the cerebral cortex. Acetylcholine (Ach) release in the cortex is causally related to awake states, again characterized by cortical field potentials with relatively less power at low frequencies and more power at high frequencies. To test whether the basal-cortical connections under investigation in these monkeys contained cholinergic projections, the Neurochip-2 was programmed to deliver a tetanic burst of electrical stimuli (500 ms train at 100 Hz) to a BF electrode every 10 minutes while continuously recording from ipsilateral cortical sites. If ACh was released, then those stimulus bursts that occurred during slow-wave sleep should cause desynchronization of the cortical slow waves (i.e. decreased low-frequency power) [15-16]

Figure 4A shows an example of a tetanic burst to BF while recording from SMA during slow-wave sleep in monkey C. The stimulation caused a transient desynchronization that lasted for 4-5s. To summarize the results across the entire recording session, the PSD was computed for the window 1s before bursts and 1s after bursts. The average PSD after the burst had less power below 20Hz relative to the average PSD before the burst (Fig. 4B). A post-stimulus decrease in 5-10 Hz power of ipsilateral cortex was obtained when stimulating either left or right BF in monkey C (Fig. 4C, black) and the right BF in monkey K (Fig. 4C, gray). In each session, the change in low-frequency power was significant (t test, $p < 0.01$). Therefore, the basal-cortical connections likely involved cholinergic fibers. Below we discuss the implications of this on the state-dependent EEP results.

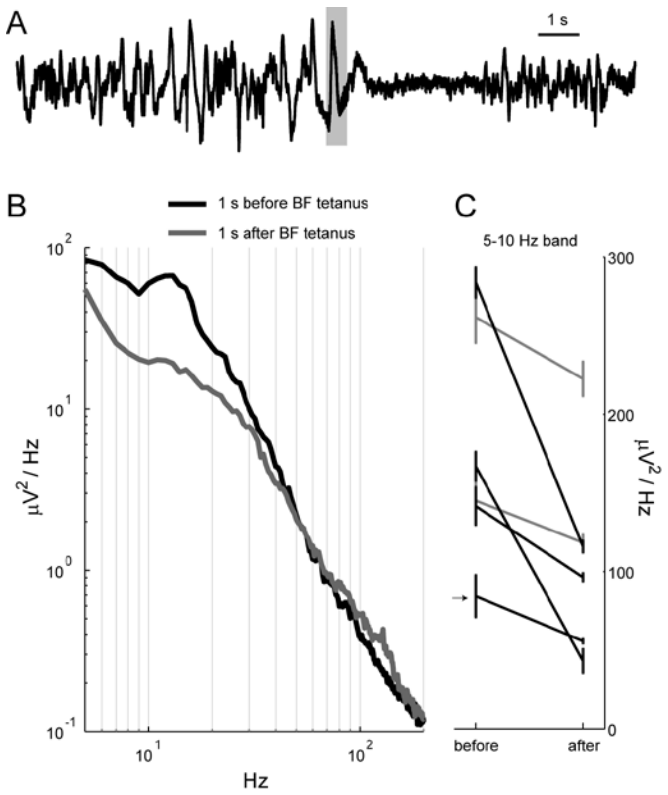

Fig. 4. BF stimulation causes cortical desynchronization. (A) Recording of SMA right during slow-wave sleep. The gray box indicates the timing of a 500-ms stimulus burst to BF right. The BF stimulation transiently abolished the slow waves in SMA. (B) Summary of overnight BF right stimulation every 10 min while recording SMA right. Black trace is the mean PSD calculated in 1-s windows before each burst. Gray trace is the mean PSD calculated in 1-s windows after each burst. BF stimulation decreased low frequency power. (C) Stimulus-induced change in 5-10 Hz power for all sessions (black = monkey C; gray = monkey K). Error bars indicate the standard error on the mean 5-10 Hz power. Arrow indicates the session shown in B.

IV. Discussion

In this study we used EEPs, measured by a portable stimulus-recording system, to document instantaneous effective neural connectivity during free behavior in the primate. The observed EEP-based connectivity patterns agreed well with what would be expected from anatomical connections. Homologous cortical areas generally have stronger callosal connections than heterologous areas [9]. Also, there are strong reciprocal connections between ipsilateral SMA and M1 [17]. Finally, the basal forebrain projects to the ipsilateral cerebral cortex, including M1 and SMA [18]. However, an EEP does not always imply a direct anatomical connection. Volume conduction of field potentials from remote sources can produce misleading results [12]. Here, we minimized the likelihood of this by using differential bipolar recording, with 0.5-mm separation between electrodes, to measure local potentials.

Our main objective was to use the Neurochip-2 to document fluctuations in EEP amplitude across the 24-h sleep-wake cycle. We found that the cortico-cortical EEP amplitude increased during the sleep state. This result is consistent with literature on sleep-wake changes in sensory-evoked potentials in the cerebral cortex. Visual [19], somatosensory [20], and auditory [21] evoked potentials are generally larger during slow-wave sleep than during wakefulness. Synchronized thalamocortical activity is thought to give rise to the slow waves recorded at the cortex during sleep. Sensory stimuli, which are relayed through thalamic nuclei, are thought to evoke a resonant response in this synchronized circuit resulting in larger evoked potentials [22]. Conversely, the more asynchronous discharge of neurons in wakefulness and REM sleep would result in smaller evoked potentials. We could not accurately identify REM states in this study without oculographic or myographic signals, but some of the variability in the EEP during the night was almost certainly related to these different sleep states. Whether resonance in synchronized thalamocortical circuits also explains the enhanced cortico-cortical EEPs during slow-wave sleep is less clear. The cortico-cortical EEPs could theoretically involve cortico-thalamic-cortical pathways. But the latencies of EEP components analyzed in this study were relatively short and more likely the result of orthodromic or antidromic excitation of intercortical pathways. Thus the size of the EEP could reflect the level of excitability at the stimulated and/or the recording site. The mechanism for the state-dependent, cortico-cortical EEP changes remains a subject for future work.

In contrast to the cortico-cortical EEPs, the basal-cortical EEPs essentially vanished during slow-wave sleep. Subsequent investigation with the Neurochip-2 revealed that the basal forebrain stimulation likely activated cholinergic neurons. Cholinergic basal forebrain neurons discharge in high-rate bursts during wakefulness and REM sleep, but stop firing almost entirely during slow-wave sleep [23]. The observed state-dependent changes in the basal-cortical EEP could be explained by the basal forebrain neurons being strongly hyperpolarized during slow-wave sleep, and thus being less responsive to the stimulus. This hypothesis emphasizes the fact that EEP changes do not necessarily imply synaptic weight changes. As demonstrated in a number of non-invasive stimulation studies, stimulus effects are contingent on the level of background neural activity at the time of stimulation [24-25].

In summary, we confirmed that the EEP is a useful measure of connectivity in the monkey. We also characterized the changes in the EEP throughout a 24-hr cycle using a novel, head-mounted electrophysiology system. Importantly, these state-dependent changes were recorded during free behavior rather than restraining or tethering the animal for long periods of time. The methods used in this study could be useful for tracking the effects of conditioning stimuli designed to artificially alter connectivity provided that the confounding factor of changing brain state is controlled.

ACKNOWLEDGMENT

We thank Dr. Matthew Edwardson for surgical assistance, Mr. Larry Shupe for programming the Neurochip-2, Ms. Olivia Robinson for helpful discussions on sleep states and Dr. Norman Weinberger for helpful discussions on nucleus basalis.

REFERENCES

[1] E. B. Plow, J. R. Carey, R. J. Nudo *et al.*, "Invasive cortical stimulation to promote recovery of function after stroke: a critical appraisal," *Stroke*, vol. 40, no. 5, pp. 1926-31, 2009.

[2] A. Jackson, J. Mavoori, and E. E. Fetz, "Long-term motor cortex plasticity induced by an electronic neural implant," *Nature*, vol. 444, no. 7115, pp. 56-60, 2006.

[3] J. M. Rebesco, and L. E. Miller, "Enhanced detection threshold for in vivo cortical stimulation produced by Hebbian conditioning," *J Neural Eng*, vol. 8, no. 1, pp. 016011, 2011.

[4] J. M. Rebesco, I. H. Stevenson, K. P. Kording *et al.*, "Rewiring neural interactions by micro-stimulation," *Front Syst Neurosci*, vol. 4, 2010.

[5] K. Stefan, E. Kunesch, L. G. Cohen *et al.*, "Induction of plasticity in the human motor cortex by paired associative stimulation," *Brain*, vol. 123 Pt 3, pp. 572-84, 2000.

[6] J. L. Taylor, and P. G. Martin, "Voluntary motor output is altered by spike-timing-dependent changes in the human corticospinal pathway," *J Neurosci*, vol. 29, no. 37, pp. 11708-16, 2009.

[7] M. N. Thabit, Y. Ueki, S. Koganemaru *et al.*, "Movement-related cortical stimulation can induce human motor plasticity," *J Neurosci*, vol. 30, no. 34, pp. 11529-36, 2010.

[8] D. McCreery, V. Pikov, and P. R. Troyk, "Neuronal loss due to prolonged controlled-current stimulation with chronically implanted microelectrodes in the cat cerebral cortex," *J Neural Eng*, vol. 7, no. 3, pp. 036005, 2010.

[9] H. J. Curtis, "Intercortical connections of corpus callosum as indicated by evoked potentials," *J Neurophysiol*, vol. 3, pp. 407-413, 1940.

[10] R. Matsumoto, D. R. Nair, E. LaPresto *et al.*, "Functional connectivity in human cortical motor system: a cortico-cortical evoked potential study," *Brain*, vol. 130, no. Pt 1, pp. 181-97, 2007.

[11] T. Paus, "Inferring causality in brain images: a perturbation approach," *Philos Trans R Soc Lond B Biol Sci*, vol. 360, no. 1457, pp. 1109-14, May 29, 2005.

[12] W. Skrandies, H. Wassle, and L. Peichl, "Are field potentials an appropriate method for demonstrating connections in the brain?," *Exp Neurol*, vol. 60, no. 3, pp. 509-21, 1978.

[13] S. Zanos, A. G. Richardson, L. Shupe *et al.*, "The Neurochip-2: an autonomous head-fixed computer for recording and stimulating in freely behaving monkeys," *IEEE Trans Neural Syst Rehabil Eng*, vol. 19, no. 4, pp. 427-35, 2011.

[14] K. J. Miller, E. C. Leuthardt, G. Schalk *et al.*, "Spectral changes in cortical surface potentials during motor movement," *J Neurosci*, vol. 27, no. 9, pp. 2424-32, 2007.

[15] S. J. Cruikshank, and N. M. Weinberger, "In vivo Hebbian and basal forebrain stimulation treatment in morphologically identified auditory cortical cells," *Brain Res*, vol. 891, no. 1-2, pp. 78-93, 2001.

[16] R. Metherate, C. L. Cox, and J. H. Ashe, "Cellular bases of neocortical activation: modulation of neural oscillations by the nucleus basalis and endogenous acetylcholine," *J Neurosci*, vol. 12, no. 12, pp. 4701-11, 1992.

[17] G. Luppino, M. Matelli, R. Camarda *et al.*, "Corticocortical connections of area F3 (SMA-proper) and area F6 (pre-SMA) in the macaque monkey," *J Comp Neurol*, vol. 338, no. 1, pp. 114-40, 1993.

[18] M. M. Mesulam, E. J. Mufson, A. I. Levey *et al.*, "Cholinergic innervation of cortex by the basal forebrain: cytochemistry and cortical connections of the septal area, diagonal band nuclei, nucleus basalis (substantia innominata), and hypothalamus in the rhesus monkey," *J Comp Neurol*, vol. 214, no. 2, pp. 170-97, 1983.

[19] H. K. Meeren, E. L. Van Luijtelaar, and A. M. Coenen, "Cortical and thalamic visual evoked potentials during sleep-wake states and spike-wave discharges in the rat," *Electroencephalogr Clin Neurophysiol*, vol. 108, no. 3, pp. 306-19, 1998.

[20] F. Z. Shaw, S. Y. Lee, and T. H. Chiu, "Modulation of somatosensory evoked potentials during wake-sleep states and spike-wave discharges in the rat," *Sleep*, vol. 29, no. 3, pp. 285-93, 2006.

[21] S. Tian, H. Qi, J. Wang *et al.*, "Differential amplitude modulation of auditory evoked cortical potentials associated with brain state in the freely moving rhesus monkey," *Neurosci Lett*, vol. 331, no. 3, pp. 159-62, 2002.

[22] A. M. Coenen, "Neuronal activities underlying the electroencephalogram and evoked potentials of sleeping and waking: implications for information processing," *Neurosci Biobehav Rev*, vol. 19, no. 3, pp. 447-63, 1995.

[23] M. G. Lee, O. K. Hassani, A. Alonso *et al.*, "Cholinergic basal forebrain neurons burst with theta during waking and paradoxical sleep," *J Neurosci*, vol. 25, no. 17, pp. 4365-9, 2005.

[24] T. O. Bergmann, M. Molle, M. A. Schmidt *et al.*, "EEG-guided transcranial magnetic stimulation reveals rapid shifts in motor cortical excitability during the human sleep slow oscillation," *J Neurosci*, vol. 32, no. 1, pp. 243-53, 2012.

[25] B. N. Pasley, E. A. Allen, and R. D. Freeman, "State-dependent variability of neuronal responses to transcranial magnetic stimulation of the visual cortex," *Neuron*, vol. 62, no. 2, pp. 291-303, 2009.

Andrew G. Richardson received the B.S.E. degree in Biomedical Engineering from Case Western Reserve University, Cleveland, OH, in 2000, and the S.M. degree in Mechanical Engineering and the Ph.D. degree in Biomedical Engineering from the Massachusetts Institute of Technology (MIT), Cambridge, MA, in 2003 and 2007, respectively.

He was a Postdoctoral Associate at MIT in 2007-2008 and is currently a Senior Fellow at the University of Washington, Seattle, WA. His research interests include motor learning, neuroplasticity, and neuromodulation

Eberhard E. Fetz received a B.S degree in Physics from the Rensselaer Polytechnic Institute, Troy, NY in 1961, and a Ph.D. degree in Physics from MIT in 1966. He is currently Professor of Physiology and Biophysics and Adjunct Professor of Bioengineering at the University of Washington, Seattle, WA. He is also a Core Staff member of the Washington National Primate Research Center in Seattle.

His primary research interest is neural mechanisms of volitional control of limb movements in behaving primates. His current research is focused on applications of bidirectional implantable brain-computer interfaces.